Electroactive Nanowires Based on Simple 4,5-Bis(dodecylthio)- and 4,5-Bis(octadecylthio)-4′,5′-bis(methoxycarbonyl)tetrathiafulvalenes

Yusuke Kobayashi, Masashi Hasegawa, Hideo Enozawa, and Masahiko Iyoda*
Department of Chemistry, Graduate School of Science and Engineering, Tokyo Metropolitan University, Hachioji, Tokyo 192-0397

(Received February 20, 2007; CL-070192; E-mail: iyoda-masahiko@c.metro-u.ac.jp)

4,5-Bis(dodecylthio)- and 4,5-bis(octadecylthio)-4′,5′-bis(methoxycarbonyl)tetrathiafulvalenes (**1a** and **1b**) exhibit gelling ability for hexane, cyclohexane, decalin, and diethyl ether to form electroactive fibrous material with 5–10 μm diameters. The doping of bunches of fibers with iodine shows moderate electrical conductivities ($\sigma_{rt} = 2.9 \times 10^{-3}$–$2.0 \times 10^{-5}$ S cm^{-1}).

A simple and effective construction method for electroconductive molecular wires is of considerable current interest, because these nanowires is one of the fundamental requirements for the fabrication of molecular electronic devices.[1] By considering the high electric conductivities of radical salts derived from tetrathiafulvalene (TTF),[2] amphiphilic TTF derivatives are a promising candidate for constructing conductive molecular wires. Using this concept, molecular wires containing TTF segments have been recently constructed and their redox properties have been explored by several groups.[3,4] However, there have been few reports on molecular wires simply based on substituted TTF derivatives, and hence the difficulty in the preparation of molecules limits its applications. Since TTF derivatives with long alkyl chains self-aggregate to show semiconductive properties via the so-called "fastener effect,"[5] the amphiphilic TTF derivatives **1a** and **1b** with both long alkyl chains and electron-withdrawing ester groups can be expected to form molecular nanowires with high electric conductivities.

Recently, we have reported the self-assembly of large π-systems with TTF–diester segments that play an important role in self-aggregation.[3c,6] From results of our previous studies, neutral amphiphilic molecules with TTF core, such as **1a** and **1b**, can form nanowires without hydrogen-bonding sites. Although the diester **1a** has already been prepared by Martín et al. and employed by several groups for the synthesis of functional π-systems as an intermediate,[7] no remarkable property of **1a** has been reported except for its enhanced solubility. On the basis of our findings, we reexamined what to construct nanostructures based on **1a** and **1b** (Scheme 1). The diesters **1a** and **1b** were prepared by the $P(OEt)_3$-mediated cross coupling of 4,5-bis(methoxycarbonyl)-1,3-dithiole-2-one (**4**) with 4,5-bis(dodecylthio)- and 4,5-bis(octadecylthio)-1,3-dithiole-2-thiones (**3a** and **3b**) in 62 and 51% yields, respectively.[8]

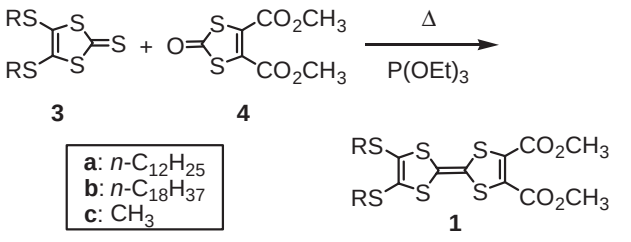

Scheme 1. Synthesis of 4,5-bis(alkylthio)-4′,5′-bis(methoxycarbonyl)tetrathiafulvalenes (**1a**–**1c**).

The ^{1}H NMR and UV–vis. spectra of **1a** and **1b** in $CDCl_3$ showed no concentration dependence presumably due to the lack of self-aggregation of these compounds in solution. Interestingly, **1a** gelated hexane at room temperature and cyclohexane, decalin, and diethyl ether at 4 °C, whereas **1b** gelated hexane, cyclohexane, decalin, and diethyl ether at room temperature. As shown in Figure 1, a warm solution of **1b** in hexane gradually changes to form a gel. Thus, **1a** showed gelling ability at relatively high concentrations (>40 mg cm^{-3}), whereas **1b** showed gelling ability at lower concentrations (>10 mg cm^{-3}).

When solvents were removed from the gel of **1a** and **1b**, fibrous xerogels were obtained (Figure 2). Microscopic images clearly show the fibrous structures of **1a** and **1b** (Figures 2b and 2c). AFM images of the fibrous materials of **1a** show entan-

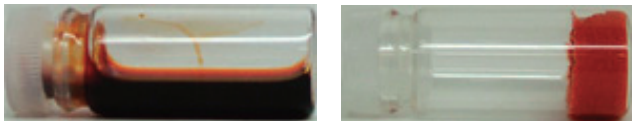

Figure 1. (a) **1b** solution (70 mg cm^{-3}) in hexane after warming at 60 °C. (b) Hexane gel of **1b** with fibrous material.

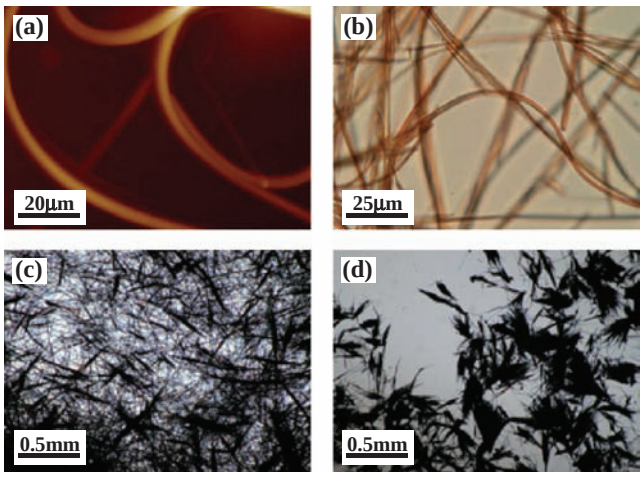

Figure 2. (a) AFM image of fibrous structure of **1a** from hexane. (b) Optical micrograph of nanowires of **1a** from hexane (1000×). (c) Optical micrograph of fibrous structure of **1b** from diethyl ether (50×). (d) Optical micrograph of nano-structure of **1b** from cyclohexane (50×).

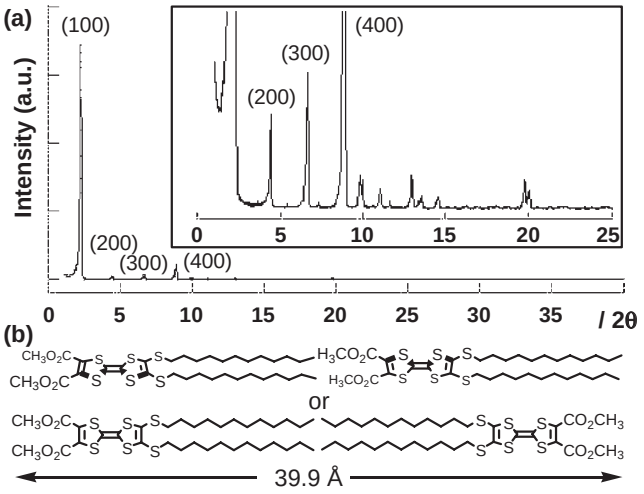

Figure 3. (a) XRD diffractogram of nanowire prepared from **1a**. A magnified diffractogram is shown in the inset. (b) Possible arrangements of molecules in **1a** wire.

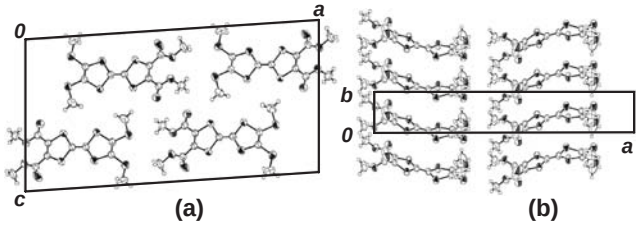

Figure 4. Crystal structure of **1c**. (a) Top view. (b) Packing diagram along *b*-axis.

gled fibrous structures with 2–5 μm diameters and 1–10 mm lengths (Figure 2a).[9] Interestingly, the nanostructures of **1b** formed in ether and cyclohexane are different (Figures 2c and 2d), and short nanowires are formed. In contrast, fibrous materials obtained from hexane have a thin and long structure, presumably due to their high ordering as compared with the nanostructures formed in ether and cyclohexane.

To obtain further information on the supramolecular self-aggregation of **1a**, an XRD analysis of its nanowires was carried out. As shown in Figure 3a, **1a** nanowires show a regular reflection pattern, and their strong (100) refection at $2\theta = 2.21^\circ$ ($d = 39.9$ Å) can be assigned to a dimeric structure with a stacked head-to-tail or head-to-head arrangement (Figure 3b). Since weak reflections at $2\theta = 4.42^\circ$ (200), 6.63° (300), and 8.84° (400) are higher-order reflections, the nanowires possess a considerably high crystallinity. The XRD pattern **1b** nanowires shows similar (100), (200), and (400) reflections, similarly reflecting a high regularity. The strong (100) reflection appears at $2\theta = 1.86^\circ$ ($d = 47.5$ Å) in accordance with the molecular size of **1b**.[10]

The X-ray crystal packing of **1c**[11] shows laterally head-to-tail dimer structures along the *a*- and *c*-axes (Figure 4a).[12] In contrast, **1c** stacks head-to-head to form a columnar structure along the *b*-axis (Figure 4b). This packing structure of **1c** may reflect the fibrous structures of **1a** and **1b** (Figure 3b).

The cyclic voltammetric (CV) analysis of the TTF–diester **1a** shows two reversible redox waves at 0.23 and 0.51 V vs Fc/Fc^+.[13] Thus, the oxidation potentials are 0.33 V higher than those of TTF, indicating the instability of the corresponding cation radical $\mathbf{1a}^{\bullet+}$ and the dication $\mathbf{2a}^{2+}$. Interestingly, the instability of the cation radical $\mathbf{1}^{\bullet+}$ can be utilized as a molecular switch. Thus, a compressed **1b** pellet shows an electric conductivity of $\sigma_{rt} = 2 \times 10^{-5}$ S cm^{-1}, doped with iodine vapor for 5 min, and the doped pellet becomes an insulator upon air. This on–off procedure can be repeated by several times without **1b** decomposition.

This work was supported in part by a Grant-in-Aid for Scientific Research on Priority Areas of Molecular Conductors (No. 15073219) from the Ministry of Education, Culture, Sports, Science and Technology in Japan. We are grateful to Prof. Hirohisa Yoshida, Mr. Takeshi Yamada, Dr. Yoshiyuki Kuwatani, and Dr. Tohru Nishinaga for helpful discussions.

References and Notes

1 a) *Molecular Switches*, ed. by B. L. Feringa, Wiley-VCH, Weinheim, **2001**. b) *Molecular Devices and Machines*, ed. by V. Balzani, M. Venturi, A. Credi, Wiley-VCH, Weinheim, **2003**. c) A. C. Benniston, *Chem. Soc. Rev.* **2004**, *33*, 573. d) D. Wouters, U. S. Schubert, *Angew. Chem., Int. Ed.* **2004**, *43*, 2480. e) R. A. Wassel, C. B. Gorman, *Angew. Chem., Int. Ed.* **2004**, *43*, 5120.

2 a) M. Bendikov, F. Wudl, D. F. Perepichka, *Chem. Rev.* **2004**, *104*, 4891. b) M. Iyoda, M. Hasegawa, Y. Miyake, *Chem. Rev.* **2004**, *104*, 5085.

3 a) J. Sly, P. Kasák, E. Gomar-Nadal, C. Rovira, L. Górriz, P. Thorarson, D. B. Amabilino, A. E. Rowan, R. J. M. Nolte, *Chem. Commun.* **2005**, 1255. b) T. Akutagawa, K. Kakiuchi, T. Hasegawa, S. Noro, T. Nakamura, H. Hasegawa, S. Mashiko, J. Becher, *Angew. Chem., Int. Ed.* **2005**, *44*, 7283. c) H. Enozawa, M. Hasegawa, D. Takamatsu, K. Fukui, M. Iyoda, *Org. Lett.* **2006**, *8*, 1917. d) M. Hasegawa, H. Enozawa, Y. Kawabata, M. Iyoda, *J. Am. Chem. Soc.* **2007**, *129*, 3072.

4 a) T. Kitamura, S. Nakaso, N. Mizoshita, Y. Tochigi, T. Shimomura, M. Moriyama, K. Ito, T. Kato, *J. Am. Chem. Soc.* **2005**, *127*, 14769. b) T. Kitahara, M. Shirakawa, S. Kawano, U. Beginn, N. Fujita, S. Shinkai, *J. Am. Chem. Soc.* **2005**, *127*, 14980. c) C. Wang, D. Zhang, D. Zhu, *J. Am. Chem. Soc.* **2005**, *127*, 16372.

5 H. Inokuchi, G. Saito, P. Wu, K. Seki, T. B. Tang, T. Mori, K. Imaeda, T. Enoki, Y. Higuchi, *Chem. Lett.* **1986**, 1263.

6 M. Iyoda, H. Enozawa, Y. Miyake, *Chem. Lett.* **2004**, *33*, 1098.

7 a) M. González, N. Martín, J. L. Segura, J. Garín, J. Orduna, *Tetrahedron Lett.* **1998**, *39*, 3269. b) J. L. Segura, E. M. Priego, N. Martín, L. Luo, D. M. Guldi, *Org. Lett.* **2000**, *2*, 4021. c) I. Olejniczak, A. Graja, A. Bogucki, M. Golub, P. Hudhomme, A. Gorgues, D. Kreher, M. Cariou, *Synth. Met.* **2002**, *126*, 263. d) M. M. S. Abdel-Mottaleb, E. Gomar-Nadal, M. Surin, H. Uji-i, W. Mamdouh, J. Veciana, V. Lemaur, C. Rovira, J. Cornil, R. Lazzaroni, D. B. Amabilino, S. De Feyter, F. C. De Schryver, *J. Mater. Chem.* **2005**, *15*, 4601.

8 For the synthesis of **1a**–**1c** and physical properties, see Supporting Information.

9 For additional optical microscopic and AFM images of **1a** and **1b**, see Supporting Information.

10 For the XRD reflactogram of nanowires of **1b**, see Supporting Information.

11 a) R. R. Schumaker, E. M. Engler, *J. Am. Chem. Soc.* **1980**, *102*, 6651. b) G. C. Papavassiliou, J. S. Zambounis, G. A. Mousdis, V. Gionis, S. Y. Yiannopoulos, *Mol. Cryst. Liq. Cryst.* **1988**, *156*, 269.

12 X-ray data for **1c**: $C_{12}H_{12}O_4S_6$, $M_r = 412.58$, space group monoclinic, $P2_1/a$ (#14), $a = 27.922(4)$ Å, $b = 4.370(3)$ Å, $c = 14.367(3)$ Å, $\beta = 93.893(14)^\circ$, $V = 1749.1(10)$ Å^3, $Z = 4$, $D_{calcd} = 1.567$ g/cm^3, $T = 298$ K, μ(Mo Kα) = 0.61 cm^{-1}, Rigaku AFC7R, Mo Kα ($\lambda = 0.71069$ Å), $R_1 = 0.039$, $R_w = 0.078$, GOF = 1.026.

13 The cyclic voltammetric analysis was carried out under the following conditions: 0.1 M *n*-Bu_4NClO_4, CH_2Cl_2, 100 mV s^{-1}, Pt working and counter electrodes, Ag/Ag^+ reference electrode, see Supporting Information.

Published on the web (Advance View) April 28, 2007; doi:10.1246/cl.2007.720